J Fluoresc
DOI 10.1007/s10895-010-0760-8

ORIGINAL PAPER

Photobleaching on Photonic Crystal Enhanced Fluorescence Surfaces

Vikram Chaudhery · Meng Lu · Cheng Sheng Huang · Sherine George · Brian T. Cunningham

Received: 20 August 2010 / Accepted: 18 October 2010

Abstract The effect of resonant fluorescent enhancement from a photonic crystal surface upon the fluorescent photobleaching rate of Cyanine-5 labeled protein has been investigated. We show that the enhanced excitation mechanism for photonic crystal enhanced fluorescence, in which the device surface resonantly couples light from an excitation laser, accelerates photobleaching in proportion to the coupling efficiency of the laser to the photonic crystal. We also show that the enhanced extraction mechanism, in which the photonic crystal directs emitted photons approximately normal to the surface, does not play a role in the rate of photobleaching. We show that the photobleaching rate of dye molecules on the photonic crystal surface is accelerated by 30x compared to an ordinary glass surface, but substantial signal gain is still evident, even after extended periods of continuous illumination at the resonant condition.

Keywords Photonic crystal · Enhanced fluorescence · Photobleaching

V. Chaudhery · C. S. Huang · B. T. Cunningham (✉)
Department of Electrical and Computer Engineering,
University of Illinois at Urbana-Champaign,
1406 W. Green St,
Urbana, IL 61801, USA
e-mail: bcunning@illinois.edu

S. George · B. T. Cunningham
Department of Bioengineering,
University of Illinois at Urbana-Champaign,
1304 W. Springfield Avenue,
Urbana, IL 61801, USA

M. Lu
SRU Biosystems,
14-A Gill St,
Woburn, MA 01801, USA

Introduction

The development of nanostructured surfaces for enhancing the electric field exposure of adsorbed fluorescent dye molecules has been a topic of intense research interest due to the potential for such surfaces to increase the detection sensitivity of surface-based fluorescent assays by over two orders of magnitude [1, 2]. Enhanced fluorescence (EF) can be applied to a broad range of assays, including gene expression microarrays [3], protein biomarker detection [4, 5], next-generation DNA sequencing [6], single molecule biophysics [7], and cell microscopy. One route towards EF has been the use of nanostructures fabricated from gold or silver, which are capable of coupling external light sources through surface plasmons to generate localized regions with electric fields exceeding the intensity of the illumination source by 10–15× [8–10]. EF using metal nanostructures is associated with relatively low resonant quality factors (Q~15), due to optical loss in the metal material, and the possibility for fluorescent quenching when dye molecules are <10 nm from the metal surface [10].

Recently, surfaces comprised entirely of dielectric materials have been demonstrated as an alternative approach for EF. Specifically, photonic crystal (PC) surfaces that are comprised of a periodically modulated grating structure that is coated over with a thin film of high refractive index material have been demonstrated to produce high quality (Q~1000) resonances and a lack of quenching effects [11]. Through selection of the grating period, a PC surface may be designed to function as an optical resonator at any desired wavelength, from ultraviolet to infrared [12, 13], and thus can be designed to interact with any fluorescent dye molecule or quantum dot [1, 2]. PC surfaces with an optical resonance designed to coincide with the wavelength of an excitation laser will

Published online: 12 November 2010

generate an enhanced electric field that is strongly confined to the PC surface and the media (air or water) immediately adjacent to the PC surface. PC "enhanced excitation" results in exposure of surface-adsorbed fluorophores to a greater electric field strength than they would otherwise experience upon an ordinary glass surface, and can be considered to be equivalent to increasing the intensity of the illumination source, but only in a region within ~100 nm of the device surface. PC surfaces may also be designed to simultaneously exhibit an optical resonance that coincides with the emission wavelength of a fluorophore. In this case, called PC "enhanced extraction," emitted photons, which would ordinarily exit the surface distributed uniformly in all directions, are spatially biased away from the PC surface at an (approximately) normal angle, so they may be gathered more efficiently by imaging objectives and/or sensors [2]. It has been shown that the processes for PC enhanced excitation and enhanced extraction operate independently, and that their overall effects multiply. Importantly, PC enhanced fluorescence (PCEF) surfaces may be produced inexpensively over large surface areas by nanoreplica molding on plastic substrates or by nanoimprint lithography on quartz substrates [14–16] so that a PC-active surface may cover an entire 1×3 in^2 slide or the bottom surface of an entire microplate.

While PCEF has been applied to gene expression microarrays and protein biomarker detection [5], the relationship between fluorescence enhancement and the rate of photobleaching has not yet been characterized. Although photobleaching may not be of critical importance for single-measurement biomolecular assays, knowledge of photobleaching effects on PC surfaces will become important as researchers attempt to apply PCs to cell-based assays and single-molecule measurements of molecular machines using FRET (Forster Resonance Energy Transfer) probes [17]. The relationship between photobleaching and fluorescent enhancement factor is not completely straightforward for PCEF because only enhanced excitation is expected to participate in photobleaching, while the enhanced extraction effect is only redirecting emitted photons for more efficient collection. Further, the angle of incidence of a single wavelength collimated illumination source is extremely important in determining the degree of enhanced excitation of the resonant modes of the PC [18]. Therefore, our goal is to characterize the rate of photobleaching from a PC surface using a collimated illumination source and to study its dependence on the angle of illumination (and thus the extent of enhanced excitation). We study PCEF using a fluorescent microscope that incorporates a collimated monochromatic light source that can be precisely tuned to the resonant illumination angle to excite the PC resonance. With this instrument, we are able to match the illumination conditions (of incident wavelength and incident angle) to satisfy the resonant condition of the PC, so the illumination is called "on-resonance." By adjusting the incident angle for a fixed wavelength so that the resonant coupling condition of the PC is not satisfied, the illumination may also be supplied in an "off-resonance" manner. We observe that the rate of photobleaching is substantially reduced when off-resonance illumination is used, and that the photobleaching rate is strongly correlated with the coupling efficiency between the PC and the illumination source, indicating that indeed only the enhanced excitation mechanism participates in modulating the photobleaching rate.

Photonic Crystal Enhanced Fluorescence

The confinement of evanescent fields to a small volume region adjacent to a surface has been previously exploited in Total Internal Reflection Fluorescence (TIRF) microscopy to reduce the levels of observable background fluorescence from the sample volume [19]. More recently, it was shown that a corrugated waveguide structure demonstrating "evanescent resonance" could enhance fluorescence excitation of dyes immobilized on the surface of a glass slide [3], thus providing elevated electric field levels to complement the surface localization of TIRF. Since that time, device structures have evolved to provide enhanced excitation with greater magnitude through resonant surfaces with narrower wavelength bands [20], combination of enhanced excitation with enhanced extraction [1], and detection instruments that more efficiently couple light into and out of the structure [18].

The PCs used in this work are nanostructures comprised of a periodically modulated low refractive index plastic/SiO_2 surface structure that is coated with a high refractive index dielectric thin film of TiO_2. The purpose of the structure is to provide an efficient optical resonator, as described in previous research [1, 2, 5, 14, 21], but summarized briefly here. The periodically modulated dielectric structure of the PC functions as a resonantly reflective optical filter, where only particular wavelength/incident angle combinations interact strongly with the structure, resulting in highly efficient reflection, while all other wavelength/incident angle combinations are transmitted through. Unlike a conventional diffraction grating, the grating period is smaller than the wavelength of light, so only the zeroth-order reflected and transmitted waves are allowed, resulting in evanescent fields with a profile that extend into the medium in contact with the PC. The resonance phenomenon is easily observed by illuminating the structure with a broad band of wavelengths and measuring the narrow bands of wavelengths that are reflected with high efficiency. The resonant condition is also dependent upon the incident angle of the external illumination, so each incident angle can have one or more

distinct resonant wavelengths. This resonance effect has been exploited to design highly efficient narrowband optical filters [22] as well as label-free optical biosensors [16]. PC resonant wavelength/angle combinations are obtained for specific polarizations of light. Transverse magnetic (TM) modes are excited when the electric field vector of illumination is oriented perpendicular to the grating lines, while transverse electric (TE) modes are excited when the electric field vector is oriented parallel to the grating lines.

The resonant modes are highly localized within and in direct proximity to the PC surface, and a large energy density is observed at these locations in the form of enhanced electromagnetic fields. The intensity of a fluorophore's emission is proportional to the electric field intensity (which is proportional to the square of the electric field) of the light exciting the molecule, so an enhanced electric field will enhance the excitation of fluorophores close to the device surface. Enhanced excitation works selectively in regions within close proximity to the PC surface due to the exponential decay of the electric field intensity from the PC into the superstrate region above the PC. Thus, enhanced excitation of the PC shares one of the advantages of TIRF microscopy because fluorophores close the substrate surface are selectively excited [9]. Rather than utilizing a TIRF microscope, a conventional confocal microarray scanner or a modified fluorescence microscope can be utilized for rapid imaging of large areas without a coupling prism. Using PC enhanced excitation, we have demonstrated fluorescence enhancement from the fluorescent dye Cyanine-5 [21] and detailed the spectral characteristics of the PC-fluorophore interaction [21] as well as the dependence on distance from the PC on enhanced excitation [11].

While enhanced excitation can be observed when the laser light incident on the PC is spectrally aligned with the resonance wavelength, another enhancement effect can be observed when a resonant mode of the PC coincides with the fluorophore emission wavelength. Enhanced extraction occurs when light emitted by fluorophores couples into this mode and is re-radiated such that it can be more efficiently gathered by the measurement instrumentation. Essentially, the PC causes some proportion of photons that would normally radiate through the substrate to be reoriented in a direction that is approximately normal to the device surface.

To perform enhanced excitation and enhanced extraction simultaneously, the PCs used in this study are designed with two separate resonances. The first is a TM resonance that coincides with the excitation wavelength of $\lambda = 632.8$ nm. The TM resonance is designed for a narrow band of wavelengths, because the electric field enhancement is proportional to the resonant quality factor, defined as $Q=\lambda/\Delta\lambda$ [23]. The second resonance is a TE mode that spectrally overlaps with the emission wavelengths of the fluorophore, where ideally the center wavelength of the TE mode coincides with the wavelength of maximum emission. The combination of these two effects has been previously used to enhance the fluorescence from semiconductor quantum dots [1] with a magnification factor of 8x for the excitation effect and 13× for the extraction effect, for an overall sensitivity enhancement of 108× [1] and additional nanostructures have been used to obtain PCEF enhancements as high as 588× [20].

Experimental

Photonic Crystal Substrate

In order to study photobleaching on substrates with fluorescence enhancement capability, a PC surface with periodic modulation in one direction was fabricated as shown in the cross-sectional diagram (not to scale) of Fig. 1 (a). The surface grating structure was formed in a ultraviolet curable polymer (UVCP) on a polyethyleneterephthalate (PET) substrate, and the polymer grating surface was coated with a 300 nm SiO_2 spacer layer followed by a high refractive index dielectric layer of TiO_2, which functions as a wave confinement layer. In order to achieve a resonance at $\lambda=632.8$ nm, electromagnetics simulation software (DiffractMOD, RSoft Design Group) based on the rigorous coupled-wave analysis (RCWA) technique was used to design the PC, resulting in a desired grating period of 360 nm and grating depth d=50 nm. Figure 1 (b) shows a top-down SEM image of a device fabricated to these design dimensions

Fabrication of the device was performed using a plastic-based nanoreplica molding process [14]. Briefly, a silicon wafer with a negative surface volume image of the desired grating pattern was fabricated using deep-UV lithography and reactive ion etching. A viscous liquid that contains an uncured monomer and a UV-activated polymerization initiator is sandwiched between a PET sheet and the silicon master wafer to enable the liquid to fill the silicon surface structure subsequent to curing with a high intensity UV lamp (Xenon, Inc). The hardened polymer grating preferentially adheres to the PET substrate, and thus can be easily peeled away from the silicon. After the molding step, the replica was cut and attached to a 1×3 in^2 microscope slide. An evaporated SiO_2 intermediate layer (t_{SiO2})=300 nm; e-beam evaporation, Denton Inc.) on the grating surface was deposited to reduce autofluorescence from the underlying polymer material due to dielectric sputtering. After the SiO_2 deposition, ~120 nm of TiO_2 was deposited by a RF sputtering system (PVD 75, Kurt Lesker) using an in-situ process monitor to accurately achieve a resonance condition

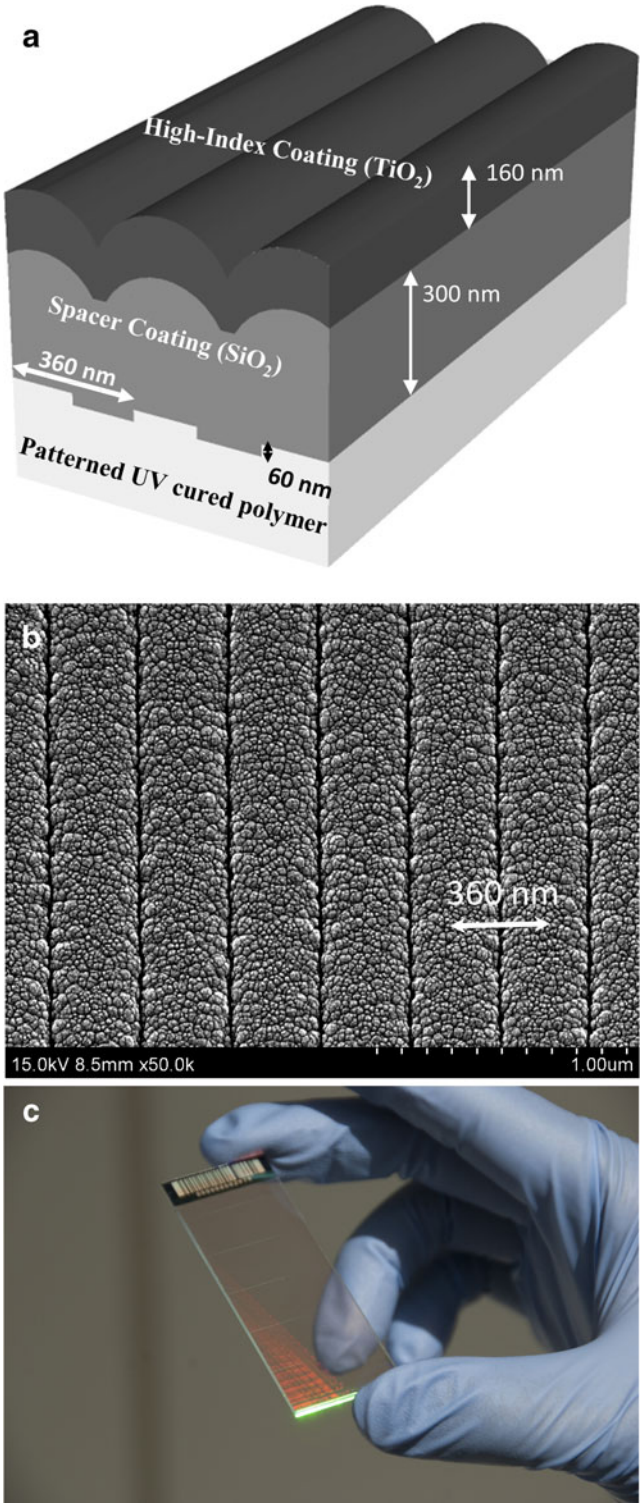

Fig. 1 Schematic cross section diagram of the photonic crystal structure (**a**), with a top view electron microscope image (**b**), and a photograph of the device attached to a standard glass microscope slide (**c**)

that nominally results in λ=633 nm wavelength resonantly coupling to the PC surface at an incident angle of 2°. Figure 1 (c) shows the final device after all fabrications steps were completed.

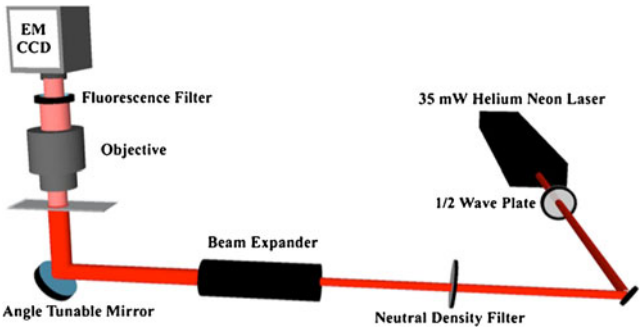

Fig. 2 Detection instrument used for photonic crystal enhanced fluorescence photobleaching study. A HeNe laser beam is expanded and collimated before reflection from an angle-tunable mirror that illuminates the photonic crystal device from below. The fluorescence emission is gathered by a conventional microscope objective and measured using a cooled EM-CCD camera

For this study we designed the PC with a TM-polarized resonance close to the Cyanine-5 (Cy5) excitation wavelength of λ=625 nm and a TE-polarized resonance spectrally overlapping the Cy5 emission spectrum centered

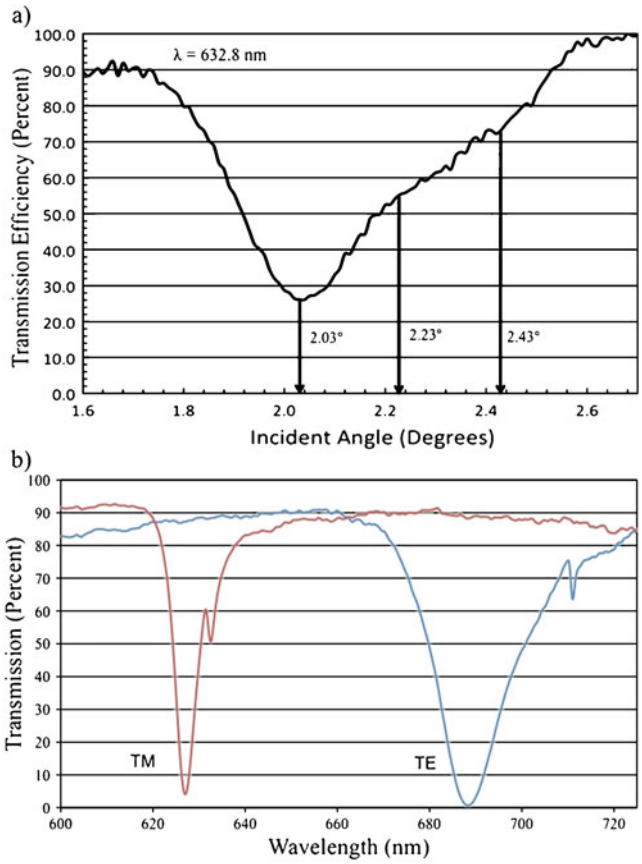

Fig. 3 Angular transmission spectrum for the TM enhanced excitation mode showing the choice of various angles of excitation **a** to generate optimal on-resonance excitation at an incident angle of 2.03°. Transmission efficiency versus wavelength **b** showing dips in transmission intensity at normal incidence for the TE (λ=690 nm) and TM (λ=625 nm) modes. Wavelengths of maximum resonance reflection correspond to wavelengths of minimum transmission

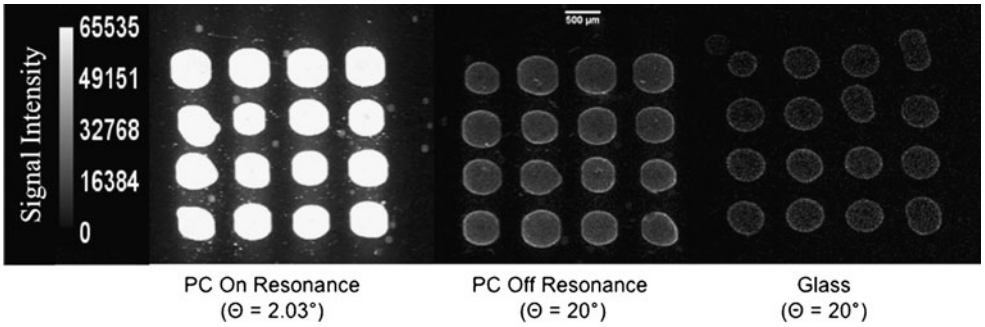

Fig. 4 Images of Cy5-streptavidin spots taken for photonic crystal on-resonance (*left*), photonic crystal off-resonance (*middle*) and an unpatterned glass slide (*right*). Images were gathered with equal exposure and camera settings for direct comparison

at λ=690 nm. The TM resonance increases the excitation of the fluorophore through enhanced electric field intensities, while the TE resonance redirects a proportion of emitted light toward the detection instrumentation. Figure 3 (b) shows the transmission spectra of the PC measured using white light illumination at normal incidence, in which dips in the transmission spectra indicate a resonance.

Detection Instrumentation

The detection system used in our study is a modified back-illuminated fluorescent microscope (Olympus BX51WI) shown schematically in Fig. 2. The microscope is equipped with a 4× objective (N.A.=0.1) and an electron multiplying CCD (C9100-13 EM-CCD; Hammamatsu Inc.) for imaging. The EM-CCD provides control over the gain settings and integration times used during the imaging process. All results reported here were measured with a sensitivity gain of 161, an analog gain of five and an exposure time of 400 ms. A 35-mW, λ=632.8 nm HeNe laser was chosen as an excitation source that was aligned with the absorption spectrum of Cy5. A high-resolution motorized gimbal-mounted mirror and beam-expanded laser provides collimated illumination at a user-selectable incident angle to the PC. In order to maintain a constant illumination area on the device, the gimbal-mounted mirror sits on top of a motorized linear stage and moves as the mirror rotates. As the collimated light at a fixed wavelength is incident on the PC surface, the angle of incidence can be tuned to allow the laser to couple with the PC resonance, thereby allowing maximum field coupling into the TM mode of the PC. The excitation illumination was TM polarized by passing the laser light through a half-wave plate.

Method

A detection experiment using a Cy5-labeled protein was carried out on the PC surface and a reference glass slide in order to directly compare the rates of photobleaching. The PC surface and the glass slide were pre-cleaned with O_2 plasma for 5 min. Following the cleaning, both PC and glass were functionalized by overnight incubation in an enclosed glass container with 5% 3-glycidoxypropyldimethylethoxysilane in dry toluene at 100 °C. After incubation the silanized devices were cleaned by sonication in toluene, methanol and deionized (DI) water and then dried under a nitrogen stream. Cy5 conjugated streptavidin (GE Healthcare) at 10 μg/ml was spotted onto the slides by a piezo dispenser (Piezorray, Perkin Elmer) to produce 4×4 arrays of labeled protein spots of ~500 μm diameter. After overnight incubation, the devices were washed by gently dipping them in a protein blocking buffer (Phosphate buffered saline at pH 7.4 with Kathon antimicrobial agent) solution for 60 s. followed by DI water rinse.

To perform measurements using the detection system in Fig. 2, we first tuned the excitation laser to the resonant angle without exposing the fluorophores. Next, we opened a shutter and captured 400 image frames in sequence, exposing the sample each time for 400 ms. The shutter was closed and reopened before each measurement so as to avoid unnecessary exposure to light. All measurements were taken on the same sample from identical spots. In order to discern the effect of enhanced excitation on the photobleaching rate, we recorded data from the angle of maximum excitation (on-resonance), minimum excitation

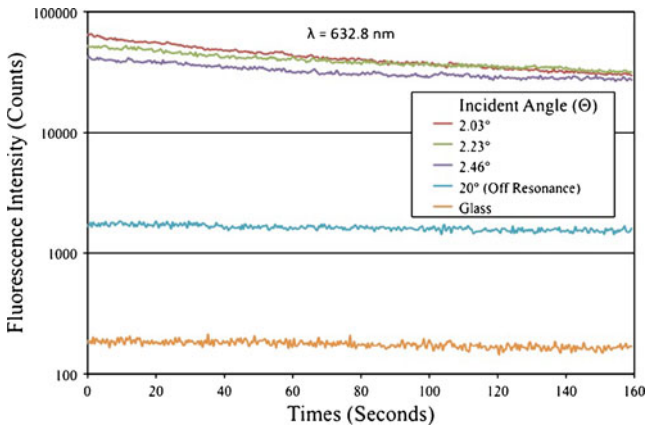

Fig. 5 Plot of the measured fluorescence intensity versus time for continuous exposure at different angles of incidence for the excitation light

Table 1 Photobleaching decay rates and signal intensity gain as pertaining to excitation angle

Device	Angle of excitation	Photobleaching decay rate 'A'	Signal intensity gain 'B'
PC	2.03°	0.0030	346.71
PC	2.23°	0.0020	279.65
PC	2.46°	0.0010	223.40
PC	20.00°	0.0001	9.13
Glass	20.00°	0.0001	1

(off-resonance) and several intermediate angles. The transmission efficiency of the selected points is shown in Fig. 3 (a). We selected angles of 20°, 2.46°, 2.23° and 2.03° where the transmission efficiency of the PC is 100%, 76%, 52% and 26% (minimum transmission) respectively.

Results

Figure 4 shows initial (first exposure) fluorescent images of Streptavidin-Cy5 spots on the PC at 2.03° (on-resonance), 20° (off-resonance) and on the glass slide illuminated at 20°. The spots shown in Fig. 4 clearly indicate enhanced excitation and enhanced extraction effects that also become evident when we analyze the numerical data.

Figure 5 shows the fluorescent intensities collected for each angle over a period of 159 s. Each curve was measured at a different angle of excitation (and same excitation wavelength of λ=632.8 nm), starting with a fresh, unexposed array of spots. The output intensity on a set of 16 spots was recorded and averaged for each frame. The background value for each frame was then subtracted to give the final averaged spot intensity. The final data are plotted on the same scale for comparison. The highest raw signal value is for the angle pertaining to the lowest transmission efficiency, corresponding to maximum resonant coupling of the excitation laser with the PC surface. As expected the curve corresponding to the 52% transmission (2.23°) has the next highest raw signal value followed by the curve corresponding to 76% transmission (2.46°). Note that even when the PC is illuminated at an angle that is far from the resonant condition (20°), we still obtain greater signal output compared to a glass surface. This high signal output is due to the enhanced extraction effect.

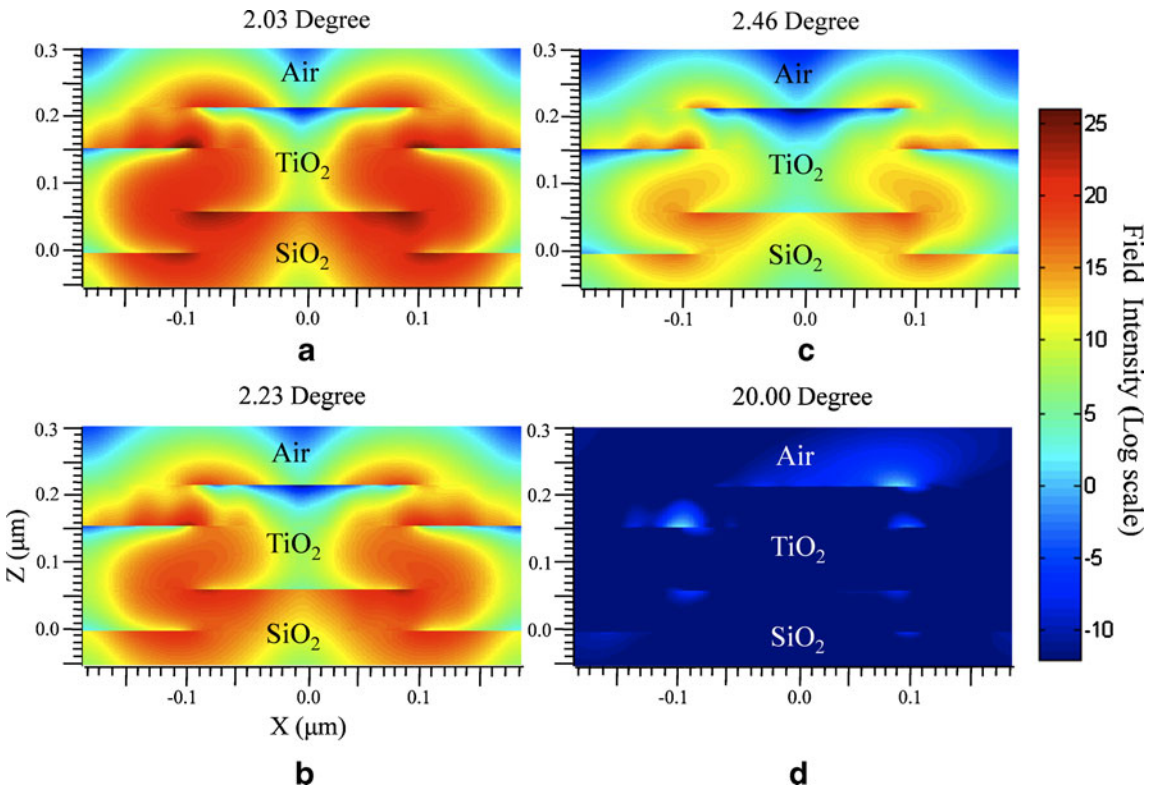

Fig. 6 Electric field intensity plots generated using rigorous coupled wave analysis for excitation conditions corresponding to 2.03° (**a**), 2.23° (**b**), 2.46° (**c**) and 20° (**d**). The electric field in the medium directly adjacent to the photonic crystal surface is modeled to be more than two orders of magnitude higher in the on-resonance (2.03°) condition, compared to the off-resonance (20°) condition

In order to compare the rates of photobleaching on the PC, we normalized each data set to our unpatterned glass control and fitted each resulting curve to an exponential function. The fitting equation used was as follows:

$$\text{Signal\_Intensity} = B^{*}e^{-A^{*}t} \quad (1)$$

where A and B are fitting parameters indicative of the photobleaching decay rate and signal intensity gain.

Table 1 lists the values of parameters A and B for different excitation angles. We observed that as we moved from the on-resonance case to the off-resonance case, there was a steady decrease in signal intensity gain and the photobleaching decay rate. Thus for higher degrees of enhancement we see a greater rate of photobleaching. This trend can be attributed to the strength of the electric fields present close to the surface at various angles.

In order to further investigate the effect more fully, we analyzed spatial plots of electric field intensity (close to the surface of the PC) obtained by rigorous coupled wave analysis (RCWA) electromagnetic field computer simulation (Rsoft, DiffractMod). Figure 6 shows cross section plots of the electric field at the four different angles of excitation. We observe that the field intensity is also directly related to the degree of coupling with the resonant mode (highest field for the on-resonance case). The increase in the electric field intensity helps explain the reason for a higher enhancement and subsequent faster rate of photobleaching. For a higher electric field intensity, a greater amount of energy will be delivered to the fluorophores located near the surface thus producing a higher fluorescence signal output.

It is important to note here that even though the rate of photobleaching is 30× higher for the PC on resonance when compared to unpatterened glass (as indicated in Table 1), after hundreds of individual exposures, a 186× enhancement factor is still observed relative to measuring the same fluorophore on a glass surface after the final scan, compared to a 346× enhancement factor for the initial scan. In fact, in order to extrapolate to mathematically determine how long of an exposure would be required to eliminate the benefits of the PC, we can equate the respective fitting equations (Eq. 1) for the PC on resonance and glass cases:

$$B_{2.03^{\circ}}{}^{*}e^{-A_{2.03^{\circ}}{}^{*}t} = B_{glass}{}^{*}e^{-A_{glass}{}^{*}t} \quad (2)$$

Inputting the respective values for constants A and B from Table 1 in the cases for the PC on resonance and the glass, we find that for the fluorescence signal for the PC on resonance to equal the fluorescence signal on the glass slide, both substrates would have to be subjected to constant exposure from the excitation laser for over 2,000 s. Thus for all practical experimental time frames, the fluorescence signal for the PC on-resonance will be higher than the fluorescence signal from an unpatterened glass substrate.

An interesting point to highlight here is that even though the signal intensity for the off-resonance case is 9× higher than the case for glass, the rate of photobleaching remains unchanged. This is a direct consequence of the extraction effect of a PC surface. The ability of the PC to allow emitted light to couple to a resonant mode and be directed towards the collection lens allows for a high degree of enhancement of the signal without adversely affecting the rate of photobleaching.

Conclusion

In this work, we have correlated the rate of fluorescent photobleaching in PC with the level of resonant fluorescent enhancement. Accelerated fluorescent photobleaching rates in a resonantly excited PC are a direct consequence of the enhancing of the surface localized electric fields exposed to adsorbed fluorescent dye molecules. This mechanism of enhanced excitation for PCEF, accelerates photobleaching in proportion to the coupling efficiency of the laser to the photonic crystal. The enhanced extraction mechanism of the PC, however, provides no contribution to the rate of photobleaching but still has significant contribution to the net signal enhancement.

Acknowledgements This work was supported by National Institutes of Health (Grant No. GM086382A), the National Science Foundation (Grant No. CBET 07-54122), and SRU Biosystems. Any opinions, findings, conclusions, or recommendations expressed in this material are those of the authors and do not necessarily reflect the views of National Institutes of Health or the National Science Foundation.

References

1. Ganesh N, Zhang W, Mathias PC, Chow E, Soares JANT, Malyarchuk V, Smith AD, Cunningham BT (2007) Enhanced fluorescence emission from quantum dots on a photonic crystal surface. Nat Nanotechnol 2:515–520
2. Ganesh N, Block ID, Mathias PC, Zhang W, Malyarchuk V, Cunningham BT (2008) Leaky-mode assisted fluorescence extraction: application to fluorescence enhancement biosensors. Opt Express 16:21626–21640
3. Budach W, Neuschaefer D, Wanke C, Chibout S-D (2003) Generation of transducers for fluorescence-based microarrays with enhanced sensitivity and their application for gene expression profiling. Anal Chem 75:2571–2577
4. Jin H, Zangar RC (2009) Protein modifications as potential biomarkers in breast cancer. Biomark Insights 4:191–200
5. Mathias PC, Ganesh N, Cunningham BT (2008) Application of photonic crystal enhanced fluorescence to a cytokine immunoassay. Anal Chem 80:9013–9020

6. Shendure J, Ji HL (2008) Next-generation DNA sequencing. Nat Biotechnol 26:1135–1145
7. Okumus B, Arslan S, Fengler SM, Myong S, Ha T (2009) Single molecule nanocontainers made porous using a bacterial toxin. J Am Chem Soc 131:14844–14849
8. Fu Y, Lakowicz JR (2006) Enhanced fluorescence of Cy5-labeled DNA tethered to silver island films: fluorescence images and time-resolved studies using single-molecule spectroscopy. Anal Chem 78:6238–6245
9. Challener WA, Edwards JD, McGowan RW, Skorjanec J, Yang Z (2000) A multilayer grating-based evanescent wave sensing technique. Sens Actuators, B 71:42–46
10. Kummerlen J, Leitner A, Brunner H, Aussenegg FR, Wokaun A (1993) Enhanced dye fluorescence over silver island films: analysis of the distance dependence. Mol Phys: An International Journal at the Interface Between Chemistry and Physics 80:1031–1046
11. Ganesh N, Mathias PC, Zhang W, Cunningham BT (2008) Distance dependence of fluorescence enhancement from photonic crystal surfaces. J Appl Phys 103:083104
12. Ganesh N, Cunningham BT (2006) Photonic crystal near UV reflectance filters fabricated by nano replica molding. Appl Phys Lett 88:071110–071113
13. Ohtera Y, Onuki T, Inoue Y, Kawakami S (2007) Multichannel photonic crystal wavelength filter array for near-infrared wavelengths. J Lightwave Technol 25:499–503
14. Block ID, Chan LL, Cunningham BT (2006) Photonic crystal optical biosensor incorporating structured low-index porous dielectric. Sens Actuators B 120:187–193
15. Block ID, Pineda MF, Choi CJ, Cunningham BT (2008) High sensitivity plastic-substrate photonic crystal biosensor. IEEE Sensors 8:1546–1547
16. Cunningham BT, Lin B, Qiu J, Li P, Pepper J, Hugh B (2002) A plastic colorimetric resonant optical biosensor for multiparallel detection of label-free biochemical interactions. Sens Actuators B 85:219–226
17. Roy R, Hohng S, Ha T (2008) A practical guide to single-molecule FRET. Nat Meth 5:507–516
18. Block ID, Mathias PC, Ganesh N, Jones SI, Dorvel BR, Chaudhery V, Vodkin LO, Bashir R, Cunningham BT (2009) A detection instrument for enhanced-fluorescence and label-free imaging on photonic crystal surfaces. Opt Express 17:13222–13235
19. Axelrod D (1981) Cell surface contacts illuminated by total internal reflection rluorescence. J Cell Biol 89:141–145
20. Wu HY, Zhang W, Mathias PC, Cunningham BT (2010) Magnification of photonic crystal fluorescence enhancement via TM resonance excitation and TE resonance extraction on a dielectric nanorod surface. Nanotechnology 21:125203–125210
21. Mathias PC, Ganesh N, Zhang W, Cunningham BT (2008) Graded wavelength one-dimensional photonic crystal reveals spectral characteristics of enhanced fluorescence. J Appl Phys 103:094320
22. Dobbs D, Cunningham BT (2006) Optically tunable photonic crystal reflectance filter. Appl Opt 45:7286–7293
23. Purcell EM (1946) Spontaneous emission probabilities at radio frequencies. Phys Rev 69:681–681